Diagnostics and Processing Applications of Electron Beam-Generated Plasmas Produced in Nitrogen

S.G. Walton, D. Leonhardt, and R.F. Fernsler, Plasma Physics Division,
US Naval Research Laboratory, Washington, DC

ABSTRACT

The Naval Research Laboratory has developed a plasma processing system for use in a variety of materials processing applications ranging from etching to deposition. The plasma in this system is produced by high-energy (≈ 2 keV) electron beams and has properties that separate it from conventional plasma sources, making it well-suited for a number of applications. In this paper, these attributes are discussed for plasmas produced in pure and diluted nitrogen backgrounds used in nitriding and plasma enhanced physical vapor deposition.

INTRODUCTION

The Naval Research Laboratory has developed a materials processing system based on electron beam-generated plasmas for use in range of processing applications [1]. When high-energy (≈ 2 keV) electron beams are used as the primary ionization source, the resultant plasmas have unique characteristics when compared to conventional low-pressure plasma sources:

Localized and scalable plasma source. The dimensions of the plasma source are tied to the electron beam dimensions which makes scaling straightforward. The beam thickness and width are determined by the electron beam source and the length is determined by the beam energy and operating pressure. For pressures of 100 mTorr and beam energies of 2 keV, the range is about 1 m. Futhermore, the plasma production region is limited to the beam volume, which is well defined and uniform when the beam is magnetically collimated. (Fields of approximately 150 gauss are sufficient to minimize beam spreading in 1 m systems.) Outside the beam channel, the plasma density and ion composition are altered by ion-electron and ion-neutral reactions, so electrodes (or substrates) can be independently positioned to take advantage of the changes in the outwardly diffusing flux of ions. This is in contrast to conventional discharges, where the boundaries of the ionization region are not well defined and increasing the dimensions in a uniform manner can be problematic.

Efficient and controllable ion production. To understand the differences between conventional sources and the use of high-energy electron beams consider Figure 1. Conventional plasma discharges rely on externally applied electric fields to raise the plasma electron temperature so that a fraction are energetic enough to ionize the gas and sustain the plasma. A maxwellian electron energy distribution is shown in Figure 1 for a typical discharge with an electron temperature of 4 eV. In such discharges, inelastic collisions (excitation/dissociation) consume most of the delivered energy and ion production favors the species with the lowest ionization potential. For multi-kilovolt electrons passing through a gas, ionization is always the dominant interaction, with the cross-sections being similar for most gases. Thus, little energy is consumed by non-ionizing collisions and species generation can be directly regulated by adjusting the background gas concentrations.

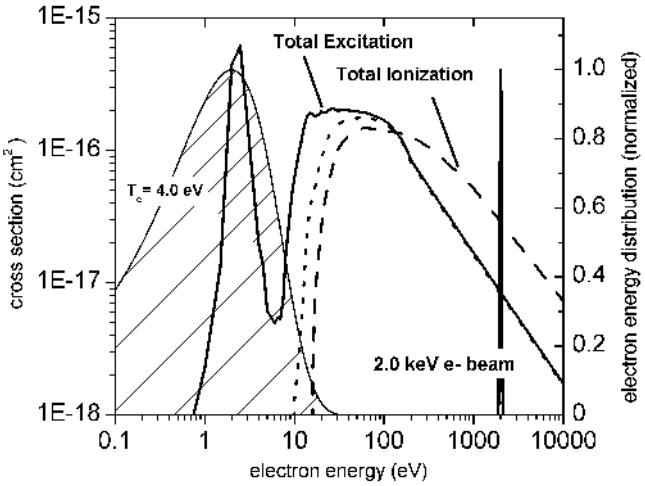

Figure 1: Electron impact cross sections in Nitrogen. Shown are the total excitation (solid), dissociation (dot), and total ionization (dash) cross sections. Also included is an approximate electron energy distribution for a discharge with a plasma electron temperature of 4 eV and a 2 keV electron beam.

Low electron temperature. Because the high-energy electron beam ionizes the gas and there is no heating applied to the plasma electrons, plasma electrons are rapidly cooled by inelastic collisions. (Electrostatic cooling also reduces the electron temperature, which is particularly important in noble gases.) The resulting plasma electron temperatures in all gases are found to be ≤ 1 eV [2], depending on the background gas. The temperature in molecular gas backgrounds tends to be lower than in noble gases due to the availability of low-energy excitation states. In the case of nitrogen, the lowest excitation levels are a few tenths of an eV [3]. Since the electron temperature determines the plasma potential [4], ions incident to

© 2006 Society of Vacuum Coaters 505/856-7188
49th Annual Technical Conference Proceedings (2006) ISSN 0737-5921

grounded surfaces will also exhibit low energies [5], typically below 5 eV.

These attributes can be advantageous in a number of processing applications [6]. In particular, systems used for stainless steel nitriding [7] and reactive sputter deposition of TiN [8] have shown unique results. Although those processing results will not be directly covered in this paper, diagnostics of similar plasmas will be presented and the key features will be noted.

EXPERIMENT

The experimental apparatus has been discussed previously [9] and is shown in the schematic of Figure 2. The system vacuum was maintained by a 2000 l/s turbo pump, with a base pressure on the order of 10^{-7} Torr. The operating pressure was achieved by introducing high-purity gases through mass flow controllers and throttling the turbo pump using a manual gate valve. The electron beam was produced by applying a 2 kV pulse to a linear hollow cathode for a selected pulse duration and duty.

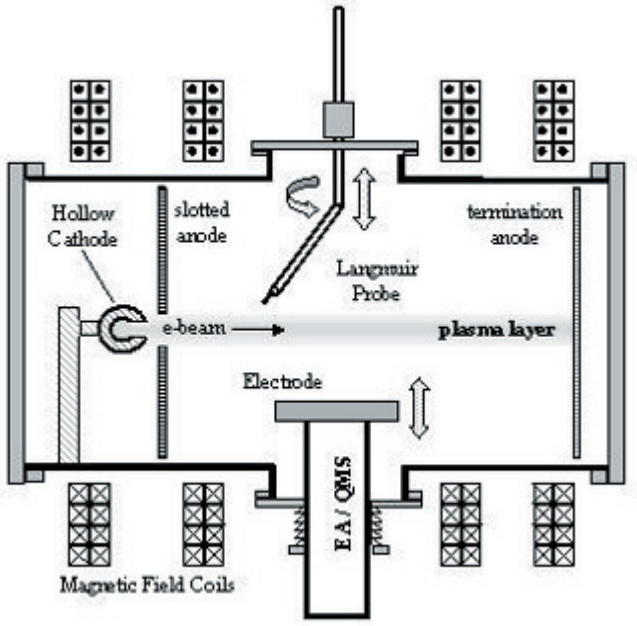

Figure 2: A schematic diagram of the processing system and diagnostic apparatus.

The emergent beam passed through a slot in a grounded anode and was then terminated at a second grounded anode located further downstream. The electron beam volume between the two anodes defines the ionization source volume, with the dimensions set by the slot size (1 cm x 25 cm) and the anode-to-anode length (43 cm). Beam spreading from collisions with the neutral background was largely eliminated by a co-axial magnetic field of 150 Gauss that was produced by a set of external magnetic field coils.

Ion energy distributions and fluxes were measured at the center of a grounded 5.7 cm diameter stainless steel electrode using a Hiden EQP 300 Plasma Probe. Ions enter the EQP through a 20 μm diameter aperture located in the center of the electrode and are first energy selected by an electrostatic energy analyzer (EA) and then mass filtered by a quadrupole mass spectrometer (QMS). The energy analyzer has a fixed resolution ($\Delta E/E_t$) that provides an uncertainty in energy of approximately $\pm$ 0.15 eV. Because the system is pulsed, all data acquisition is time resolved and the gating techniques have been described elsewhere [10]. The EQP has not been calibrated to determine the absolute flux of each species, so the intensity of the measured signal is reported in arbitrary units.

The plasma electron temperature T_e and plasma density n_p were determined using a Langmuir probe that was mounted on a multi-motion feedthrough and constantly heated with an internal resistive element to reduce surface contaminants. Time-resolved probe techniques entailed stepping the probe voltage in discrete intervals and recording the current as a function of time at each voltage. The characteristic I-V trace was then generated at each time, and the values of T_e and n_p were derived from a best fit of the I-V trace to a Maxwellian electron energy distribution.

RESULTS AND DISCUSSION

Plasmas Produced in Pure Nitrogen

Electron beam generated plasmas produced in pure nitrogen have been used in reactive sputter deposition of TiN films. [8] In that work, the electron beam generated plasma was produced between the magnetron and the growing film. The pressure was lower ($\approx$ 30 mTorr) than the results presented here and of course, differences in bulk plasma and ion flux at the substrate will be different because of the magnetron-generated plasma. Nonetheless, the results here are valuable in understanding the addition of the electron beam generated plasma.

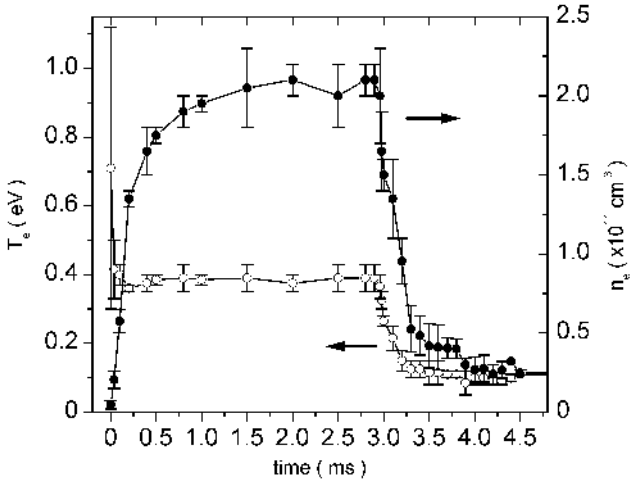

Figure 3: Time-resolved n_p and T_e measurements in a plasma produced in pure nitrogen. The measurements were made on the axis of the electron beam.

Shown in Figure 3 are the results of Langmuir probe measurements made in 50 mTorr of pure nitrogen with the plasma modulated using a 3 ms pulse at a 10% duty. The probe was located on the electron beam axis. The plasma can be characterized by three distinct phases, which include the initiation, steady state, and afterglow. The initiation phase shows a high electron temperature and low plasma density, the steady state is characterized by a nearly constant T_e and n_p, and the afterglow exhibits a collapse in both. These phases are common to any pulsed plasma or discharge; what is unique to this data is the low T_e and high plasma density achieved during the steady state.

Ion energy distributions measured at a grounded electrode located 2.5 cm from the electron beam axis are shown in Figure 4. The energy distributions and mass spectrum were accumulated during a gate that spanned the entire width of the pulse (3 ms). The energy distributions are characterized by low maximum and most probable energies indicative of low plasma potentials resulting from the low electron temperatures. N_2^+ was the dominant species at this position, with N^+ comprising about 35-40% of the ion flux. The N^+ flux contribution is high compared to most discharges and slightly higher than the expected production ratio of 4:1 for electron energies of 2 keV. However, electron-ion recombination ($e^- + N_2^+ \rightarrow 2$ N) is a strong gas phase reaction in these plasmas since T_e is very low ($k_r \sim 10^{-7}\ T_e^{-0.39}$ cm^3/s [11]) and is responsible for the comparatively low N_2^+ ion flux.

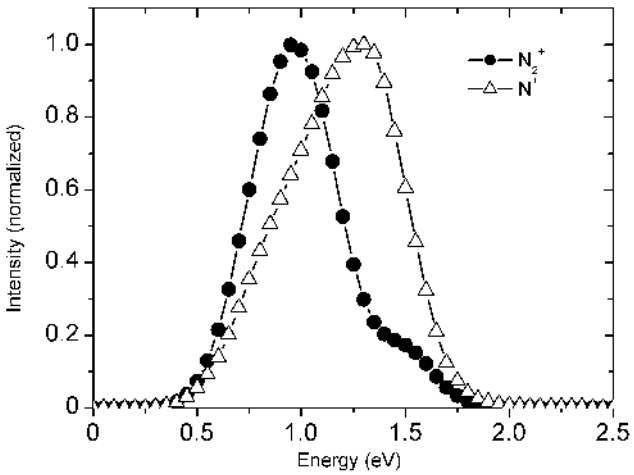

Figure 4: Normalized ion energy distributions measured in plasma produced in pure nitrogen. The electrode was located 2.5 cm from the electron beam axis.

Plasmas Produced in Diluted Nitrogen

Shown in Figure 5 are the relative ion fluxes as a function of time for plasmas produced in 160 mTorr nitrogen/argon mixtures (12% Ar). The pulse width was 1 ms and the duty factor is 50%. These same conditions were used in stainless steel nitriding. [7] The slight delay in time is due to the ion time of flight in the EQP. The temporal variation in the total ion flux is in agreement with the change in plasma density seen in Figure 3 and thus generally similar to other pulsed discharges. The relative ion fluxes however are worth noting, particularly the dominance of the N^+ ion in the afterglow. This results from the rapid destruction of N_2^+ ions via the electron-ion recombination reaction noted above. The destruction of atomic ions is either diffusive, which is typically slow, or via charge exchange ($Ar^+ + N_2 \rightarrow Ar + N_2^+$; $k_r \sim 10^{-11}$ cm^3/s [12] and $N^+ + N_2 \rightarrow N + N_2^+$; $k_r \sim 10^{-12}$ cm^3/s [13]). Given the large difference in destruction rates, it is not surprising that the atomic nitrogen dominates in the afterglow.

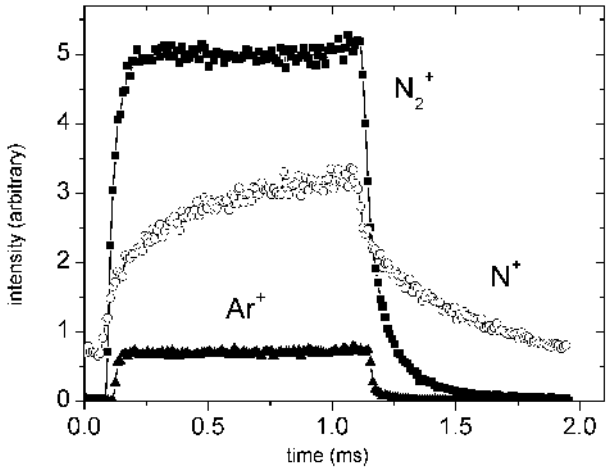

Figure 5: Time-resolved ion fluxes sampled from plasmas produce in mixtures of nitrogen and argon measured at an electrode located 2.5 cm from the electron beam axis.

The influence of these gas phase reactions was also demonstrated spatially, as seen in Figure 6, where the relative ion fluxes as a function of electrode position are shown. The data was acquired using the same conditions as in Figure 5 and accumulated over the entire period. The beam axis is located at x=0 and the approximate width extends to 0.5 cm on the abscissa. The relative flux of Ar^+ ions is between 5% and 10% when the electrode is closest to the beam. This is slightly less than the relative argon gas concentration (12%) but again, gas phase reactions likely reduce the Ar^+ ion density as a function of distance from the beam.

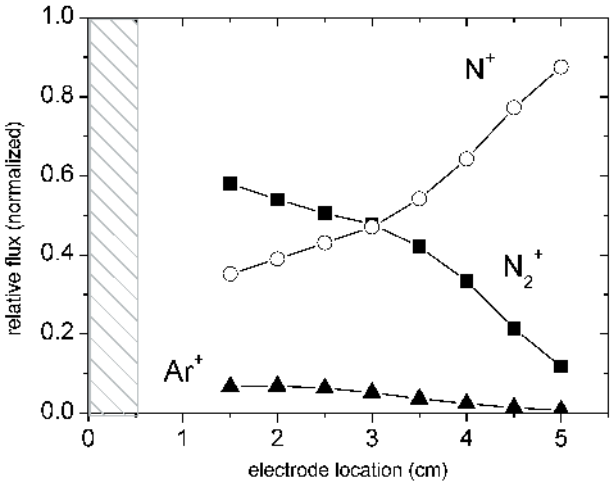

Figure 6: Relative ion fluxes sampled from plasmas produced in mixtures of nitrogen and argon measured as a function of electrode location.

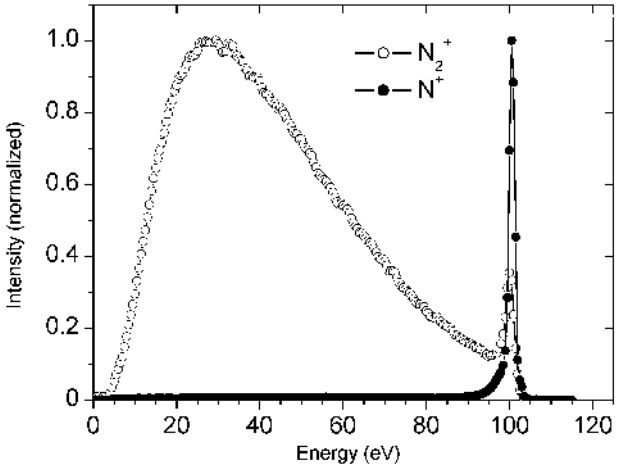

Figure 7: N_2^+ and N^+ ion energy distributions measured at an electrode located 2.5 cm from the electron beam axis for plasma produced in nitrogen/argon mixtures. The electrode was ground but the termination anode was biased to +100 V.

If the temporal and spatial variations of the relative ion fluxes are considered, these results demonstrate a unique ability to tailor the relative ion fluxes by varying the pulse width, duty cycle, or substrate to source distance. Specifically, we note the abundance of atomic nitrogen ions in the afterglow and with increasing distance. It is possible therefore, to regulate the incident atomic ion flux using straightforward adjustments of the operating parameters. Such adjustments were found to affect the nitriding rate for stainless steel. [14]

There are a number of benefits to having large N^+ ion densities and fluxes. In Figure 7, where the energy distributions of both the molecular and atomic ions are shown for the same plasma as in Figures 5 and 6, but the termination anode was biased to +100 V to produce a high-voltage sheath at the ground electrode of the EQP. "Floating" the plasma is equivalent to putting a –100 V bias on the electrode. The reasons for the difference in distributions is related to the collisionality of each species as it transverses the sheath. Specifically, the mean free path of N_2^+ ions (~ 0.05 cm) is shorter than the sheath thickness (~ 0.1 cm) while the mean free path of N^+ ions (1 cm) exceeds it. [14] Thus, the N^+ ion can realize the full voltage drop across the sheath and since the plasma potential is low, a large fraction of incident ions will impact the surface with an energy commensurate with the applied bias.

SUMMARY

Investigations designed to determine the bulk plasma properties and ion fluxes at adjacent electrodes in pulsed, electron beam-generated plasmas produced in pure and diluted nitrogen were discussed. The electron temperature and plasma density were determined as function of time and the ion flux was measured as a function of time and electrode location. The electron temperature during the steady state is approximately 0.4 eV and the plasma density is on the order of 10^{11} cm^{-3}. The incident ion flux is characterized by low energies (0.5-2.0 eV). The relative N^+ ion flux was found to be greater than 30% at all electrode locations. Because the plasma is pulsed, all measured values are found to be time-dependent and the relative ion flux is also found to be dependent on electrode location.

The results demonstrate some of the unique features of materials processing systems based on these plasmas. The plasma density is comparable to most plasma processing systems although the electron temperature, incident ion energies, and relative flux intensities are difficult to achieve using discharges operating at similar pressures and source-to-substrate distances. The spatio-temporal variation in the total and relative ion flux at electrodes located adjacent to the plasma can be used as a way to regulate ion fluxes at substrate surfaces so that, through simple adjustments in operating parameters, the flux can be tailored to optimized a given process.

ACKNOWLEDGEMENTS

This work is supported by the Office of Naval Research.

REFERENCES

1. D. Leonhardt, C. Muratore, S.G. Walton, and R.A. Meger, "Plasma Enhanced Surface Treatments Using Electron Beam-generated Plasmas," *Surf. Coat. Technol.* 188-189, 299 (2004).

2. D. Leonhardt, S.G. Walton, D.D. Blackwell, W.E. Amatucci, D.P. Murphy, R.F. Fernsler, and R.A. Meger, "Plasma diagnostics in Large Area Plasma Processing System," *J. Vac. Sci. Technol.* A 19 (4), 1367 (2001).

3. Y. Itikawa, M. Hayashi, A. Ichimura, K. Onda, K. Sakimoto, K. Takayanagi, M.Nakamura, H. Nishimura and T. Takayanagi, Cross Sections for Collisions of Electron and Photons with Nitrogen Molecules," *J. Phys. Chem. Ref. Data,* 15(3), 985 (1986).

4. M.A. Lieberman and M.J. Lichtenberg, *Principles of Plasma Discharges and Materials Processing* (John Wiley & Sons, New York, 1994).

5. S.G. Walton, D. Leonhardt, D.D. Blackwell, R.F. Fernsler, D.P. Murphy, and R.A. Meger, "Ion energy distributions in a pulsed, electron beam-generated plasma," *J. Vac. Sci. Technol.* A 19 (4), 1325 (2001).

6. D. Leonhardt, C. Muratore, S.G. Walton, D.D. Blackwell, R.F. Fernsler, and R.A. Meger, "Generation of Electron-Beam Produced Plasmas and Applications to Surface Modification," *Surf. Coat. Technol.* 177-178, 682 (2004).

7. C. Muratore, D. Leonhardt, S.G. Walton, D.D. Blackwell, R.F. Fernsler, and R.A. Meger, "Low-temperature nitriding of stainless steel in an electron beam generated plasma," *Surf. Coat. Technol.* 191, 255 (2005).

8. C. Muratore, S.G. Walton, D. Leonhardt, and R.F. Fernsler, "Control of plasma flux composition incident on TiN films during reactive magnetron sputtering and the effect on film microstructure," *J. Vac. Sci. Technol.* A, 24 (1), 25 (2006).

9. Scott G. Walton, "Characterizations of Electron Beam-Generated Plasmas for Materials Processing," *Vacuum Technology and Coating* 5 (9), 38 (2004).

10. S.G. Walton, D. Leonhardt, and R.F. Fernsler, "Time-resolved Diagnostics in a Pulsed, Electron Beam-Generated Plasma," *IEEE Trans. Plas. Sci.* 33, 838 (2005).

11. F.J. Mehr and M.A. Biondi, "Electron Temperature Dependence of Recombination of O2+ and N2+ Ion with Electrons," *Phys. Rev.*, 181, 264 (1969).

12. Y. Ikezoe, S. Matsuoka, M. Takebe, and A. Viggiano, *Gas Phase Ion-Molecule Reaction Rates Through 1986 (*published by the Ion Reaction Research Group of The Mass Spectroscopy Society of Japan; Distributed by Maruzen Co., Ltd., Tokyo, Japan, 1989).

13. S.C. Brown, *Basic data of Plasma Physics*, 2nd ed. (MIT Press, Cambridge, MA, 1996).

14. C. Muratore, S.G. Walton, D. Leonhardt, R.F. Fernsler, D.D. Blackwell, R.A. Merger, "Effect of plasma flux composition on the nitriding rate of stainless steel," *J. Vac. Sci. Technol.* A, 22 (4), 1530 (2004).